

To appear in *Optimization Methods & Software*  
 Vol. 00, No. 00, Month 20XX, 1–14

## L-BFGS Precoding Optimization Algorithm for Massive MIMO Systems with Multi-Antenna Users

Evgeny Bobrov<sup>ab\*</sup>, Dmitry Kropotov<sup>bc</sup>, Sergey Troshin<sup>c</sup> and Danila Zaev<sup>a</sup>

<sup>a</sup>*Moscow Research Center, Huawei Technologies, Russia;* <sup>b</sup>*M. V. Lomonosov Moscow State University, Russia;* <sup>c</sup>*National Research University Higher School of Economics, Russia*

*(Received 00 Month 20XX; final version received 00 Month 20XX)*

The paper studies the multi-user precoding problem as a non-convex optimization problem for wireless multiple input and multiple output (MIMO) systems. In our work, we approximate the target Spectral Efficiency function with a novel computationally simpler function. Then, we reduce the precoding problem to an unconstrained optimization task using a special differential projection method and solve it by the Quasi-Newton L-BFGS iterative procedure to achieve gains in capacity. We are testing the proposed approach in several scenarios generated using Quadriga – open-source software for generating realistic radio channel impulse response. Our method shows monotonic improvement over heuristic methods with reasonable computation time. The proposed L-BFGS optimization scheme is novel in this area and shows a significant advantage over the standard approaches. Proposed method has a simple implementation and can be a good reference for other heuristic algorithms in this field.

**Keywords:** Optimization, Massive MIMO, Precoding, SVD, L-BFGS, Interior-Point

### 1. Introduction

Wireless channels with multiple input and multiple output (MIMO) provide significantly more capacity than their counterparts with one input and one output. Thus, the MIMO system is an essential technology in modern wireless telecommunications, including Wi-Fi and 5G systems [1]. It allows using antenna array clusters to send multiple signal beams for multiple user devices simultaneously. The proper construction of such beams is called *beamforming* or *precoding* procedure [8, 11]. In the linear channel assumptions, the correct precoding is a complex matrix of the general form with given constraints, which corresponds to the physical limitations of the system.

We measure the quality of the precoding using the well-known functions such as Signal-to-Interference-and-Noise Ratio (*SINR*) and Spectral Efficiency (*SE*) [16]. In addition to these functions, the literature considers Minimum MSE (MMSE) [10, 19]) function, and the discrete Bit-Error-Rate (BER) [6] quality measure. On the basis of MMSE function the most precoding algorithms in the field are derived [2].

The standard precoding algorithms, which are well-known in the literature, are Maximum-Ratio Transmission (MRT) [9], Zero-Forcing (ZF) [20] and Regularized ZF (RZF) [17] (including its recent variant – Adaptive RZF (ARZF) [2]). All these algorithms have analytical formulas, without taking into account the target function of *SE* or do it implicitly, maximizing the numerator of *SINR* using the MRT algorithm, or reducing

---

\*Corresponding author. Email: eugenbobrov@ya.ru

the denominator of  $SINR$  using the ZF algorithm. This leads to simple but non-optimal precoding solutions. Therefore, one of our goal is to study the potential improvement of precoding methods.

While during downlink (DL) on the transmitter side a base station apply precoding matrices, symmetrically, on the receiver side users apply detection matrices. The knowledge of the detection of the user allows to construct more efficient precoding for the base station, some works even consider joint construction of precoding and detection algorithms, see e.g. [14]. In general, we don't have exact information about the user detection, but we can mean a type of it. The most common detections are well-described in the literature, such as Minimum MSE (MMSE) [10, 19] and Interference Rejection Combiner (MMSE-IRC) [13], which can be applied in order to eliminate the multiuser interference. We also utilize the recently proposed theoretical Conjugate Detection (CD) [2].

We consider the most practical formulation of the problem with multiple-antenna users [15] and per-antenna power constraints at the base station [18]. Alternatively, simpler and mathematically attractive statements include single-antenna users and single total power constraint at the base station. Thus, considered problem is constrained optimization programming with non-convex function and multiple constraints. It can be solved by using suboptimal heuristic methods [9, 20], interior point methods [5], projection-based methods [4], or any of them with reparametrization (variables transform). We find a convenient reparametrization, that reduces the problem to an unconstrained one. This reduction allows to use an advanced unconstrained gradient-based methods. The proper reparametrization is one of the main contributions of the article. Even with the right reparameterization, the target function is computationally complex and must be simplified to accelerate convergence. Proper simplification is the second and new approach presented in this article.

In this study we, firstly, approximate the  $SE$  [16] objective function using the CD matrix [2] to simplify our algorithm as much as possible. As the second step, we reduce the precoding problem to an unconstrained optimization task and solve it by the Quasi-Newton L-BFGS iterative procedure [22] to achieve the maximum possible quality. We write an end-to-end «differentiable projection»-based method, where gradients are taken both for the functional and the projection, which tends to very fast convergence of the proposed method. The problem to be solved is not convex, and so we find the local maximum of the  $SE$ .

The novelty of the proposed method consists in simplifying the objective function  $SE$ , which makes the task more attractive from a computational point of view. Secondly, the reparametrization of precoding for an unlimited task was invented. We called this parametrization *Differentiable projection*. In addition, classical parameterization using the *Softmax* function is also described.

Our parametrization method is a know-how and is designed to solve the problem of precoding. In fact, it can be generalized to other topics of constrained optimization. In combination with the simplified function, we proposed the target problem of unlimited optimization as a reference algorithm for evaluating the upper bound of quality. Finally, all our research is based on realistic power limits per antenna and multiple antenna users, which in itself is a separate problem for finding the right approach to solving.

All investigated algorithms were tested in several scenarios of Quadriga [7] - an open-source software for generating realistic radio channel impulse response. Our method shows monotonic improvement over heuristic methods with reasonable computational time.

We adopt commonly used notational conventions throughout the paper. Matrices and vectors will be denoted by bold-face upper and lower case letters, respectively. Furthermore,  $(\cdot)^H$  denotes Hermitian transpose.

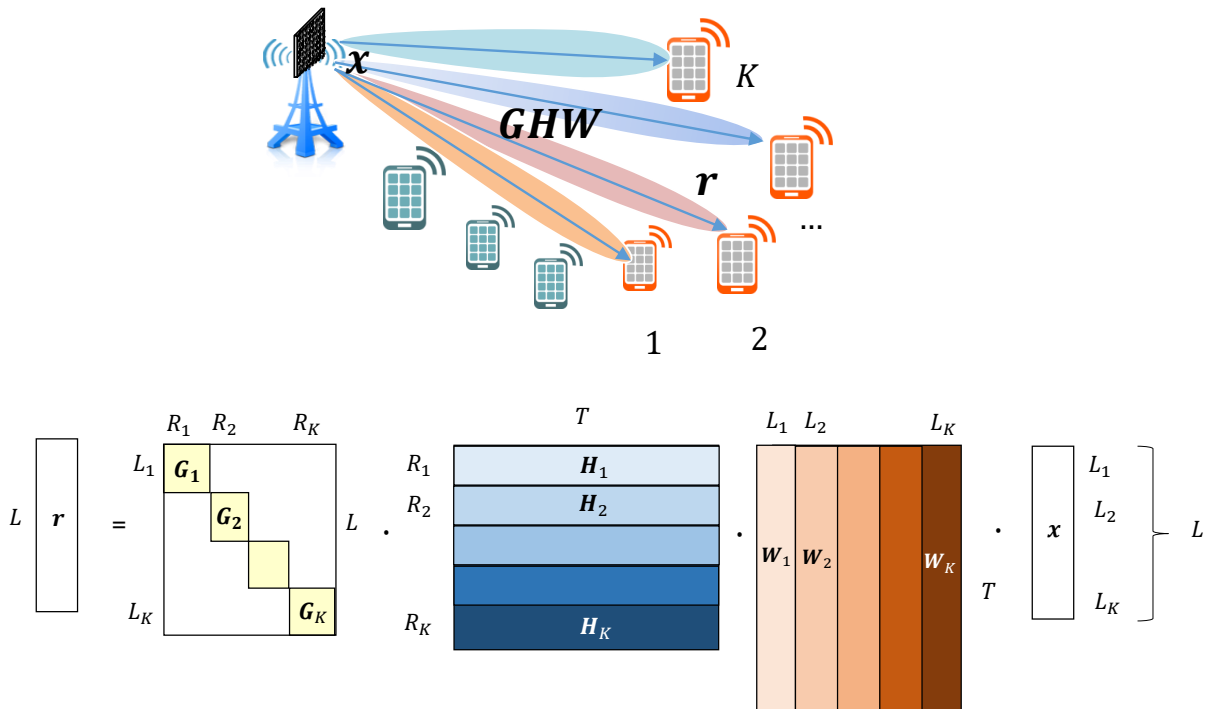


Figure 1. Multi-User Precoding allows to transmit different information to different users simultaneously. The problem is to find an optimal precoding matrix  $\mathbf{W}$  of the system given the target  $SE$  function [2] .

The paper is organized as follows. In Section 2 we describe the system model of the studied Massive MIMO network, introduce quality measures, types of detection matrices, approximated quality function, power constraints and problem statement. In Section 3 we study solutions for precoding problem, reference methods, proposed optimization solution and its relative computational complexity. In Section 4 we provide numerical results in the Quadriga radio simulator. Section 5 contains the conclusion.

## 2. System Model

In 5G cellular networks, we look at a precoding problem in multi-user massive MIMO communication. A single base station with multiple transmit antennas is used. These antennas send signals to multiple users at the same time. Each user also has multiple antennas for receiving signals. The transmission quality between the base station and the users is measured by the base station. The precoding problem entails determining an appropriate weighting (phase and gain) for transmitting the signal in order to maximise the signal power at the receivers' output.

In our system we consider  $K$  users and for  $k$ -th user we would like to transmit him  $L_k$  symbols. In total, we would like to transmit a vector  $\mathbf{x} \in \mathbb{C}^L$ , where  $L = L_1 + \dots + L_K$ . We multiply the transmitted vector by a precoding matrix  $\mathbf{W} \in \mathbb{C}^{T \times L}$ , where  $T$  is a total number of transmit antennas on a base station. Then we transmit the precoded symbols for the all users. Suppose that  $k$ -th user has  $R_k$  receive antennas and  $\mathbf{H}_k \in \mathbb{C}^{R_k \times T}$  is a channel between  $k$ -th user and the base station. Then  $k$ -th user receives  $\mathbf{H}_k \mathbf{W} \mathbf{x} + \mathbf{n}_k$ , where  $\mathbf{n}_k$  is a Gaussian noise. The noise appears as a result of thermal distortions of

the system. Finally,  $k$ -th user applies a detection of transmitted symbols by multiplying the received vector by a detection matrix  $\mathbf{G}_k \in \mathbb{C}^{L_k \times R_k}$ . The final vector of detected symbols of the all users is denoted by  $\mathbf{r} \in \mathbb{C}^L$ . The whole process of transmitting symbols is presented in Fig. 1. Note that the linear precoding and detection can be implemented by simple matrix multiplications.

Finally, the Multi-User MIMO model is described using the following linear system:

$$\mathbf{r} = \mathbf{G}(\mathbf{H}\mathbf{W}\mathbf{x} + \mathbf{n}). \quad (1)$$

Where  $\mathbf{r} \in \mathbb{C}^L$  is a *received vector*, and  $\mathbf{x} \in \mathbb{C}^L$  is a *sent vector*, and  $\mathbf{H} \in \mathbb{C}^{R \times T}$  is a *channel matrix*, and  $\mathbf{W} \in \mathbb{C}^{T \times L}$  is a *precoding matrix*, and  $\mathbf{G} \in \mathbb{C}^{L \times R}$  is a *block-diagonal detection matrix*, and  $\mathbf{n} \sim \mathcal{CN}(0, I_L)$  is a *noise-vector*. The constant  $T$  is the number of transmit antennas,  $R$  is the total number of receive antennas, and  $L$  is the total number of transmitted symbols in the system. Usually they are related as  $L \leq R \leq T$ . Each of the matrices  $\mathbf{G}, \mathbf{H}, \mathbf{W}$  decomposes by  $K$  users. The numbers  $K, L, R, T$  and channel matrix  $\mathbf{H} \in \mathbb{C}^{R \times T}$  are predefined in the system.

It is convenient [15] to represent the user channel matrix  $k$  via its reduced Singular Value Decomposition (SVD):

$$\mathbf{H}_k = \mathbf{U}_k^H \mathbf{S}_k \mathbf{V}_k, \quad \mathbf{U}_k \mathbf{U}_k^H = \mathbf{U}_k^H \mathbf{U}_k = \mathbf{I}_{R_k}, \quad \mathbf{S}_k = \text{diag}\{s_1, \dots, s_{R_k}\}, \quad \mathbf{V}_k \mathbf{V}_k^H = \mathbf{I}_{R_k}. \quad (2)$$

Where the *channel matrix* for user  $k$ ,  $\mathbf{H}_k \in \mathbb{C}^{R_k \times T}$  contains channel vectors  $\mathbf{h}_i \in \mathbb{C}^T$  by rows, the singular values  $\mathbf{S}_k \in \mathbb{C}^{R_k \times R_k}$  are sorted by descending,  $\mathbf{U}_k \in \mathbb{C}^{R_k \times R_k}$  is a unitary matrix of left singular vectors, and matrix  $\mathbf{V}_k \in \mathbb{C}^{R_k \times T}$  consists of *right singular vectors*.

Collecting all users together, we can write the following decomposition:

LEMMA 2.1 [2] Denote  $\mathbf{H} = [\mathbf{H}_1, \dots, \mathbf{H}_K] \in \mathbb{C}^{R \times T}$  the concatenation of individual channel rows  $\mathbf{H}_k$ . The following representation holds:

$$\mathbf{H} = \mathbf{U}^H \mathbf{S} \mathbf{V}. \quad (3)$$

where the  $\mathbf{H} \in \mathbb{C}^{R \times T}$ , and  $\mathbf{S} = \text{diag}(\mathbf{S}_k) \in \mathbb{C}^{R \times R}$ , and  $\mathbf{U} = \text{bdiag}(\mathbf{U}_k) \in \mathbb{C}^{R \times R}$  is block-diagonal unitary matrix, but  $\mathbf{V} = [\mathbf{V}_1, \dots, \mathbf{V}_K] \in \mathbb{C}^{R \times T}$  has a general form.

## 2.1 Quality Measures

The quality functions are based not on the actual sending symbols  $x \in \mathbb{C}^L$ , but on some distribution of them [1]. Thus, we get the common functions for all the assumed symbols, which can be sent using the specified precoding. The *Signal-to-Interference-and-Noise (SINR)* functional of the  $l = l(k)$ -th symbol and user  $k$ , is defined as:

$$\text{SINR}_l(\mathbf{W}, \mathbf{H}_k, \mathbf{g}_l, \sigma, P) = \frac{|\mathbf{g}_l^H \mathbf{H}_k \mathbf{w}_l|^2}{\sum_{i \neq l} |\mathbf{g}_l^H \mathbf{H}_k \mathbf{w}_i|^2 + \|\mathbf{g}_l\|^2 \frac{\sigma^2}{P}}, \quad \forall l \in \mathcal{L}_k, \quad (4)$$

where  $\mathbf{w}^l \in \mathbb{C}^T$  is the  $l$ -th column of the precoding matrix.

To get the formula for the  $k$ -th user *SINR*, namely the effective *SINR*, that shows the signal quality of the user, we average his  $L_k$  per-symbol *SINRs* (4) by the geometric mean:

$$SINR_k^{eff}(\mathbf{W}, \mathbf{H}_k, \mathbf{G}_k, \sigma, P) = \left( \prod_{l \in \mathcal{L}_k} SINR_l(\mathbf{W}, \mathbf{H}_k, \mathbf{g}_l, \sigma, P) \right)^{\frac{1}{L_k}}, \quad (5)$$

where the detection matrix  $\mathbf{G}_k \in \mathbb{C}^{L_k \times R_k}$  contains vector of the  $k$ -th user symbols  $\mathbf{g}_l$ .

To get the final functional of *Spectral Efficiency* we apply the Shannon's formula over all effective user SINRs (5):

$$SE(\mathbf{W}, \mathbf{H}, \mathbf{G}, \sigma, P) = \sum_{k=1}^K L_k \log_2(1 + SINR_k^{eff}(\mathbf{W}, \mathbf{H}_k, \mathbf{G}_k, \sigma, P)) \rightarrow \max_{\mathbf{W}} \quad (6)$$

The formula (6) shows the throughput capacity of the system as a whole. Now it depends on the whole channel and detection matrices  $\mathbf{H} \in \mathbb{C}^{R \times T}$  and  $\mathbf{G} \in \mathbb{C}^{L \times R}$ . We will use it as our final score function, compare algorithms and find precoding matrices  $\mathbf{W} \in \mathbb{C}^{T \times L}$ , solving the problem of maximizing this function.

Additionally, we consider the function of *Single-User SINR*:

$$SUSINR(\tilde{\mathbf{S}}, \sigma^2, P) = \frac{P}{\sigma^2} \left( \prod_{k=1}^K \frac{1}{L_k} \left( \prod_{l \in \mathcal{L}_k} s_l^2 \right)^{\frac{1}{L_k}} \right)^{\frac{1}{K}}. \quad (7)$$

The formula (7) reflects the quality of the channel for the specified user without taking into account the others. It depends on the greatest  $L_k$  singular values  $\tilde{\mathbf{S}}_k \in \mathbb{R}^{L_k \times L_k}$  of the  $k$ -th user channel matrix  $\mathbf{H}_k \in \mathbb{C}^{R_k \times T}$ . Finally, the matrix  $\tilde{\mathbf{S}} \in \mathbb{C}^{L \times L}$  contains all singular values on the main diagonal, such as  $\tilde{\mathbf{S}} = \text{diag}(\tilde{\mathbf{S}}_1 \dots \tilde{\mathbf{S}}_K) \in \mathbb{C}^{L \times L}$ . We will use this function as a universal channel characteristic in our experiments.

## 2.2 Detection Matrices

*Detection* aims to reverse the channel with precoding to an identity matrix. We study the most common forms of the *detection* matrix  $\mathbf{G}$ , which is called Minimum MSE (*MMSE*) [10], Interference Rejection Combine (*MMSE-IRC*) [13], and Conjugate Detection (*Conjugate*) (*CD*). In our work we will focus our attention on the *MMSE-IRC* and *CD* methods.

Firstly, *MMSE* detection realizes the following rule:

$$\mathbf{G}_k^{MMSE}(\mathbf{A}_k) = \mathbf{A}_k^H (\mathbf{A}_k \mathbf{A}_k^H + \lambda \mathbf{I})^{-1}, \quad \mathbf{A}_k = \mathbf{H}_k \mathbf{W}_k. \quad (8)$$

The scalar  $\lambda = \frac{\sigma^2}{P}$  is the system noise-to-signal ratio. The constant  $P$  refers to the base station power and  $\sigma^2$  refers to the system noise. Thus, the method implicitly consider the *noise* equal for all symbols:  $\mathbf{n} = \frac{\sigma^2}{P} \mathbf{1} \in \mathbb{C}^L$ , and detection  $\mathbf{G}$  which tends to eliminate it. One may notice that the use of the method requires solving a system of linear equations of the size of layers  $L$ .

Secondly, *MMSE-IRC* detection uses additional information about noise-covariance matrix  $\mathbf{R}_{uu}^k$  as follows:

$$\mathbf{G}_k^{IRC}(\mathbf{A}_k, \mathbf{R}_{uu}^k) = \mathbf{A}_k^H (\mathbf{A}_k \mathbf{A}_k^H + \mathbf{R}_{uu}^k + \lambda \mathbf{I})^{-1}, \quad \mathbf{A}_k = \mathbf{H}_k \mathbf{W}_k, \quad (9)$$

where the covariance matrix has the form as:

$$\mathbf{R}_{uu}^k = \mathbf{H}_k (\mathbf{W}\mathbf{W}^H - \mathbf{W}_k\mathbf{W}_k^H) \mathbf{H}_k^H = \mathbf{H}_k \left( \sum_{u=1, u \neq k}^K \mathbf{W}_u\mathbf{W}_u^H \right) \mathbf{H}_k^H. \quad (10)$$

LEMMA 2.2 Using the linear property, you can get the following representation of the detection matrix MMSE-IRC:

$$\begin{aligned} \mathbf{G}_k^{IRC}(\mathbf{H}_k, \mathbf{R}_{uu}^k) &= (\mathbf{H}_k\mathbf{W}_k)^H (\mathbf{H}_k\mathbf{W}_k(\mathbf{H}_k\mathbf{W}_k)^H + \mathbf{R}_{uu}^k + \lambda\mathbf{I})^{-1} = \\ &= (\mathbf{H}_k\mathbf{W}_k)^H (\mathbf{H}_k\mathbf{W}_k(\mathbf{H}_k\mathbf{W}_k)^H + \mathbf{H}_k \left( \sum_{u=1, u \neq k}^K \mathbf{W}_u\mathbf{W}_u^H \right) \mathbf{H}_k^H + \lambda\mathbf{I})^{-1} = \\ &= (\mathbf{H}_k\mathbf{W}_k)^H (\mathbf{H}_k\mathbf{W}(\mathbf{H}_k\mathbf{W})^H + \lambda\mathbf{I})^{-1}. \end{aligned} \quad (11)$$

Thirdly, *Conjugate Detection* can be written in the following form:

$$\mathbf{G}^C := \tilde{\mathbf{S}}^{-1}\tilde{\mathbf{U}} \in \mathbb{C}^{L \times R}, \quad \mathbf{G}_k^C = \tilde{\mathbf{S}}_k^{-1}\tilde{\mathbf{U}}_k \in \mathbb{C}^{L_k \times R_k}. \quad (12)$$

Where  $\tilde{\mathbf{S}}_k \in \mathbb{C}^{L_k \times L_k}$  contains the first  $L_k$  largest singular values, and  $\tilde{\mathbf{U}}_k \in \mathbb{C}^{L_k \times R_k}$  contains the first  $L_k$  corresponding singular vectors. The *Conjugate* and *MMSE-IRC* detection matrices are very closely related to each other, assuming low noise and ZF or RZF Precoding (the proof of this fact we put elsewhere). We can use the *Conjugate* detection at the base station to configure the precoding matrix assuming *MMSE-IRC* for user equipments.

### 2.3 Approximated Quality Function

Assuming the conjugated detection  $\mathbf{G}^C$  (12) we have come to the following approximated function of the *SINR* [2]:

$$SINR_l^C(\mathbf{W}, \tilde{\mathbf{v}}_l, s_l, \sigma^2, P) = \frac{|\tilde{\mathbf{v}}_l\mathbf{w}_l|^2}{\sum_{i \neq l}^L |\tilde{\mathbf{v}}_l\mathbf{w}_i|^2 + s_l^{-2} \frac{\sigma^2}{P}} \quad (13)$$

Spectral Efficiency function can be simplified in the following way, where  $\tilde{\mathbf{v}}_l \in \mathbb{C}^T$  is the singular vector of the  $l$ -th symbol, and  $s_l \in \mathbb{R}$  is the singular value of the  $l$ -th symbol:

$$\begin{aligned} SE^C(\mathbf{W}, \tilde{\mathbf{V}}, \tilde{\mathbf{S}}, \sigma, P) &= \sum_{l=1}^L \log_2(1 + SINR_l^C(\mathbf{W}, \tilde{\mathbf{v}}_l, s_l, \sigma, P)) = \\ &= \sum_{l=1}^L \log_2 \left( \sum_{i=1}^L |\tilde{\mathbf{v}}_l\mathbf{w}_i|^2 + s_l^{-2} \frac{\sigma^2}{P} \right) - \sum_{l=1}^L \log_2 \left( \sum_{i \neq l}^L |\tilde{\mathbf{v}}_l\mathbf{w}_i|^2 + s_l^{-2} \frac{\sigma^2}{P} \right) \rightarrow \max_{\mathbf{W}}. \end{aligned} \quad (14)$$

One may notice that we have completely moved away from *user antennas* of shapes  $R_k$  and  $R$  and work only with *user layers* of shapes  $L_k$  and  $L$ . The formula now does not depend on channel matrix  $\mathbf{H}_k \in \mathbb{C}^{R_k \times T}$  but on the eigenvectors of the  $l$ -th layer  $\mathbf{v}_l \in \mathbb{C}^T$ , which has length  $T$  by the number of antennas. The inversed squared singular values  $s_l^{-2} \in \mathbb{R}$  scale the noise power.

## 2.4 Power Constraints

We formulate the realistic *per-antenna power constraints* [21]. Since we have  $T$  equal transmitter antennas, the power limitation applied to each of them is  $\frac{P}{T}$ . The antenna power can be described in terms of the row norms of the precoding matrix:  $\|\mathbf{w}^m\|^2 \leq \frac{P}{T} \forall m$ .

It is clear that per-antenna constraints satisfies the total power:  $\|\mathbf{w}^1\|^2 + \dots + \|\mathbf{w}^T\|^2 \leq P$ , which is the *sum-power constraint* across all transmit antennas. While analytically attractive, such a *sum-power constraint* is often unrealistic in practice. In a physical implementation of a multi-antenna base station, each antenna has its own power amplifier in its analog front-end and is limited individually by the linearity of the power amplifier. Thus, a power constraint imposed on a *per-antenna basis* is more realistic.

## 2.5 Problem Statement

We formulate the constrained smooth optimization problem:

$$\begin{aligned} & \underset{\mathbf{W} \in \mathbb{C}^{T \times L}}{\text{maximize}} && SE(\mathbf{W}, \mathbf{H}, \mathbf{G}, \sigma, P) \\ & \text{subject to} && \|\mathbf{w}^m\|^2 \leq \frac{P}{T}, \quad m = 1 \dots T \end{aligned} \quad (15)$$

Where  $\mathbf{w}^m \in \mathbb{C}^L$  in the  $m$ -th row of the precoding matrix.

## 3. Solutions for Precoding

### 3.1 Reference Methods

The *precoding* matrix  $\mathbf{W}$  is responsible for the beamforming from the base station to the users. The linear methods for precoding do the following. Firstly, the linear solutions obtain singular value decomposition for each user  $\mathbf{H}_k = \mathbf{U}_k^H \mathbf{S}_k \mathbf{V}_k \in \mathbb{C}^{R_k \times T}$  (Lemma 2.1) and take the first  $L_k$  singular vectors  $\tilde{\mathbf{V}}_k \in \mathbb{C}^{L_k \times T}$  which attend to the first  $L_k$  greatest singular values [15]. All these matrices are concatenated to the one matrix  $\tilde{\mathbf{V}} \in \mathbb{C}^{L \times T}$ .

Finally, the precoding matrix is constructed from the obtained singular vectors. We describe linear methods for constructing a precoding matrix. We meet the power constraints using the scalar post-adjustment. We divide the precoding matrix on its maximal row norm as  $\max\{\|\mathbf{w}^t\|\}_{t=1 \dots T}$  and scale them on  $\sqrt{\frac{P}{T}}$ . Thus, the per-antenna power constraints can satisfy the following condition:  $\|\mathbf{w}^m\|^2 \leq \frac{P}{T} \forall m$ .

*Maximum-Ratio Transmission* is the simplest way of computing the precoding matrix. It takes the Hermitian conjugate of the channel singular vectors [9]:

$$\mathbf{W}_{MRT} = \mu \tilde{\mathbf{V}}^H \mathbf{P} \in \mathbb{C}^{T \times L} \quad (16)$$

Where matrix  $\mathbf{P} \in \mathbb{R}^{L \times L}$  denotes power allocation between symbols and constant  $\mu > 0$  utilizes the power constraints. In such a way, the signal beams can be sent directly to users without considering their interaction. The Maximum-Ratio approach is preferred in noisy systems where the noise power is higher than inter-user interference.

*Zero-Forcing* is the next modification of the precoding algorithm. which performs decorrelation of the symbols using inverse correlation matrix of the channel vectors [20]:

$$\mathbf{W}_{ZF} = \mu \tilde{\mathbf{V}}^H (\tilde{\mathbf{V}} \tilde{\mathbf{V}}^H)^{-1} \mathbf{P} \in \mathbb{C}^{T \times L}. \quad (17)$$

With matrix  $\mathbf{P} \in \mathbb{R}^{L \times L}$  and constant  $\mu > 0$ , which have the same meaning as in the previous section. Such precoding construction sends the signal beams to the users without creating any interference between them. Different from the previous method, the Zero-Forcing approach is preferred when the potential inter-user interference is higher than the noise power. There is a huge performance gain by eliminating the interference.

In the previous method, beams are sent not directly to the users but with some deviation, which actually reduces the payload. Thirdly, the following modification, *Regularized Zero-Forcing*, corrects the beams, which allows some inter-user interference and significantly increases the payload [17]:

$$\mathbf{W}_{RZF} = \mu \tilde{\mathbf{V}}^H (\tilde{\mathbf{V}} \tilde{\mathbf{V}}^H + \mathbf{R})^{-1} \mathbf{P} \in \mathbb{C}^{T \times L}. \quad (18)$$

Where diagonal matrix  $\mathbf{R} \in \mathbb{R}^{L \times L}$  denotes symbol *regularization* and matrix  $\mathbf{P} \in \mathbb{R}^{L \times L}$  and constant  $\mu > 0$  as the previous ones. As the baseline, we use a special form [12] of the regularization matrix  $\mathbf{R} = \frac{\sigma^2 L}{P} \mathbf{I}$ . It is the most common precoding in real practice.

Algorithm  $\mathbf{W}_{RZF}$  is a precoding with *scalar regularisation*. Finally, *Adaptive Regularized Zero-Forcing* takes into account effective noise of the system. It was proposed *Adaptive RZF (ARZF)* algorithm [2] with *diagonal matrix regularization*:

$$\mathbf{W}_{ARZF} = \mu \tilde{\mathbf{V}}^H (\tilde{\mathbf{V}} \tilde{\mathbf{V}}^H + \lambda \mathbf{S}^{-2})^{-1} \mathbf{P}, \quad \lambda = \frac{\sigma^2 L}{P}. \quad (19)$$

### 3.2 Proposed Optimization Solution

Let us introduce the following parametrization. This method explicitly constrains antenna rows using (sub-)differentiable projection on a ball as a part of the Conjugate Spectral Efficiency function:

$$\underset{\mathbf{W} \in \mathbb{C}^{T \times L}}{\text{maximize}} \quad \mathcal{S}(\text{proj}_{P,T}(\mathbf{W})), \quad (20)$$

where  $\mathcal{S}(\mathbf{W})$  is defined assuming *CD*  $\mathcal{S}(\mathbf{W}) = SE^C(\mathbf{W}, \tilde{\mathbf{V}}, \mathbf{S}, \sigma, P)$  or assuming *MMSE-IRC* detection  $\mathcal{S}(\mathbf{W}) = SE(\mathbf{W}, \mathbf{H}, \mathbf{G}^{IRC}(\mathbf{W}), \sigma, P)$  and

$$\text{proj}_{P,T}(\mathbf{W}) = \begin{cases} \mathbf{w}^m, & \|\mathbf{w}^m\|^2 \leq \frac{P}{T} \\ \frac{\mathbf{w}^m}{\|\mathbf{w}^m\|} \sqrt{\frac{P}{T}}, & \|\mathbf{w}^m\|^2 > \frac{P}{T}, \quad \forall m = 1 \dots T \end{cases} \quad (21)$$

with  $\mathbf{w}^m \in \mathbb{C}^L$  in the  $m$ -th row of the precoding matrix.

*Remark 1* We also add maximization of the target *SE* function for reference.

*Remark 2* As the starting point, we are using Regularized  $\mathbf{W}_{RZF}$  or Adaptive  $\mathbf{W}_{ARZF}$ .

The key feature of the proposed method is that the optimization process, on the one hand, always remains within the feasible range and at the same time can be solved using unconstrained optimization methods, such as quasi-Newton methods. In contrast to the

projection gradient method, the iteration solution always remains in a feasible area and does not need an explicit projection on the boundary. Moreover, in the particular case the projection-based method doesn't converge appropriately. And the same for interior point method: its basic realisation doesn't give an appropriate solution for our task. An advantage of the proposed method is that it seeks the solution on the boundary (and we know that the optimum is on the boundary). This search within the such complicated edge is possible using the Quasi-Newton L-BFGS method [22].

---

**Algorithm 1:** On the optimal precoding matrix and Quasi-Newton L-BFGS [22]

---

**Input:** Channel singular vectors  $\tilde{\mathbf{V}}$ ,  
channel singular values  $\mathbf{S}$ , station power  $P$ , noise  $\sigma^2$ , iterations  $N$ ,  
Tolerance grad  $\varepsilon_g$ , termination tolerance on first order optimality (default: 1e-5),  
Tolerance change  $\varepsilon_c$ , termination tolerance on function value and parameter changes  
(default: 1e-9).  
**Initialize** precoding matrix  $\mathbf{W} \leftarrow \mathbf{W}_0$ ;  
**for**  $t = 1$  **to**  $N$  **do**  
    **if** *True conditions on  $\varepsilon_g$  or  $\varepsilon_c$*  **then**  
        | **return**  $\text{proj}_{P,T}(\mathbf{W})$   
    **end**  
    Calculate the gradient:  $\nabla_{\mathbf{W}} \mathcal{S}(\text{proj}_{P,T}(\mathbf{W}))$ ;  
    Find the optimal direction recursively:  $\mathbf{D} = \mathbf{D}(\nabla_{\mathbf{W}} \mathcal{S}(\text{proj}_{P,T}(\mathbf{W})))$ ;  
    Find the optimal step length  $\alpha = \arg \max_{\alpha} \mathcal{S}(\text{proj}_{P,T}(\mathbf{W} + \alpha \mathbf{D}))$ ;  
    Make the optimization step:  $\mathbf{W} \leftarrow \mathbf{W} + \alpha \mathbf{D}$ ;  
**end**  
**return**  $\text{proj}_{P,T}(\mathbf{W})$

---

We consider  $\mathcal{S}(\mathbf{W})$  assuming *CD* or assuming *MMSE-IRC* detection, and also initial precoding matrix in the form of *RZF* or *ARZF*. By this way, we compare four options:

- (1) QN CD RZF      (2) QN CD ARZF      (3) QN IRC RZF      (4) QN IRC ARZF

### 3.3 Relative Computational Complexity

The complexity of our algorithm is no more than  $\sim 3Nx$  times higher than the baseline *RZF*. On each iteration of *QNS* we have to compute gradient  $\nabla SE^C(\mathbf{W})$  of  $x$  complexity and adjust step length  $\alpha$ , which takes roughly two calls of the function  $SE^C(\mathbf{W})$  of  $2x$  total complexity (see the Table 1).

### 3.4 Alternative Optimization Solution

For comparison, let us consider the classic softmax parametrization of the precoding matrix (this is an option of interior point approach). It turned out that such parametrization leads to the same solution as the differentiable projection method, but the latter converges at

RZF	$SE^C(\mathbf{W})$	$\nabla SE^C(\mathbf{W})$	N-iterations of <i>QNS</i>
$x$	$x$	$x$	$\sim 3Nx$

Table 1. Relative computational complexity.

least twice as fast as softmax. We believe that this is due to the fact that most constraints should be up to the boundary, and softmax parameterization arguments in this sense should have the value of infinity. So, we marked the softmax method as an alternative method and brought it here for a better understanding of the solvable problem.

$$\underset{\mathbf{W} \in \mathbb{C}^{T \times L}}{\text{maximize}} \quad SE^C(\mathbf{W}, \tilde{\mathbf{V}}, \mathbf{S}, \sigma, P) \quad (22)$$

$$\mathbf{W} = \{w_{ij}\}_{i,j=1}^{T,L}, \quad w_{ij} = \rho_{ij} \exp(i\phi_{ij}), \quad \rho_{ij} \in \mathbb{R}_+, \quad \phi_{ij} \in [0, 2\pi) \quad (23)$$

$$\rho_{ij}^2 = \frac{\exp(\theta_{ij})}{\sum_{k=1}^L \exp(\theta_{ik})} \frac{\sigma(\alpha_i)P}{T}, \quad \phi_{ij} = 2\pi\sigma(\eta_{ij}) \quad (24)$$

Where  $\sigma(\cdot)$  means a sigmoid function, and  $\{\theta_{ij}, \eta_{ij}, \alpha_i\}$  are free parameters that can take any real values. Thus, in another way we can reduce the problem of optimizing precoding with constraints to the problem without constraints.

#### 4. Numerical Experiments

The main scenario is Urban Non-Line-of-Sight 3GPP\_38.901\_RMa\_NLOS [3] (Fig. 4). We model users in the urban landscape. We are testing the proposed approach in several scenarios generated using Quadriga [7] - open-source software for generating realistic radio channel impulse response. For each scenario we generate 40 different channel matrices  $\mathbf{H} \in \mathbb{C}^{n_{users} \times 4 \times 64}$ . The carrier frequency for each channel matrix is selected randomly over the bandwidth. User selection is described in the next section. The base station antenna array forms a grid with 8 placeholders along the  $y$  axis and 4 placeholders along the  $x$  axis. The receiver antenna array consists of two placeholders along the  $x$  axis. Each placeholder contains two cross-polarized antennas. An interested reader can find detailed hyperparameters for antenna models and generation processes in table 3 (see Appendix). All unlisted Quadriga parameters are those set by default. We describe the generation process in detail in our work [2].

For each scenario we generate 40 different channels:  $\mathbf{H} \in \mathbb{C}^{K \times R_k \times T}$ :

- $T = 64$  base station antennas,
- $K = 8$  users,
- $R_k = 4$  user antennas,
- $L_k = 2$  user layers.

##### 4.1 Qualitative Results

For each generated channel seed, we fix station power  $P = 1$  and select system noise  $\sigma^2$  for the specified  $SUSINR$  (7) average value. We use binary search to select the noise  $\sigma^2$  since  $SUSINR$  depends on it monotonically. We report the hyper-parameters for Quadriga in the Table 3.

The results of the comparison are in Figure 2 and Table 2. In all cases the final  $SE$  function is calculated using MMSE-IRC detection (9), geometric mean effective SINR (5) and Shannon's capacity (6).

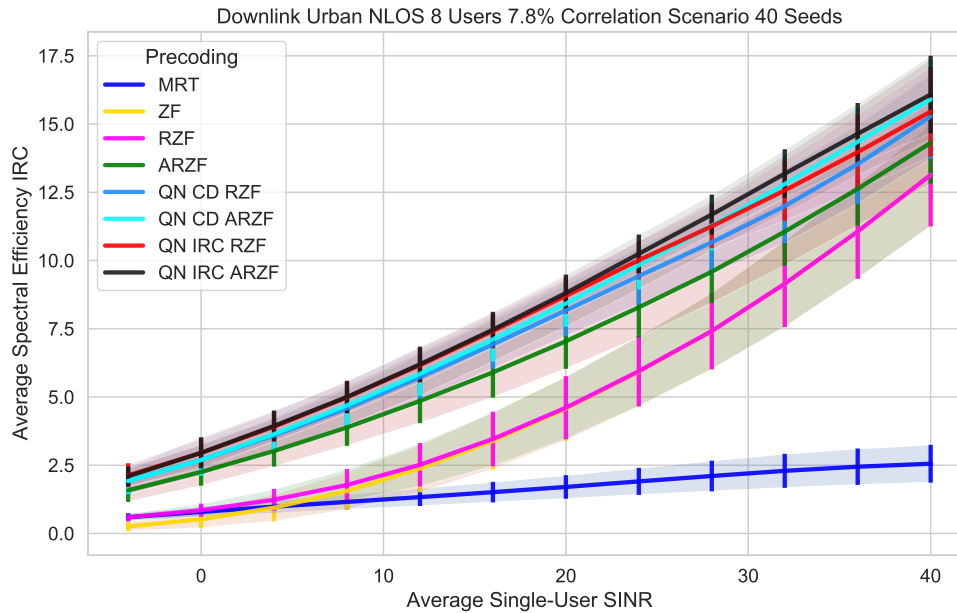


Figure 2. Urban NLOS 8 Users. The graph shows IRC Spectral Efficiency of the different precoding algorithms.

To begin with, the experimental results in Figure 2 and Table 2 show that all gradient-based methods starting with "QN," which stands for "Quasi-Newton" (Algorithm (1)), outperform heuristic algorithms such as MRT (16), ZF (17), RZF (18), and ARZF (19).

The second keyword "CD" and "IRC" stands for the assumed detection algorithm: Conjugate Detection (14) and MMSE-IRC (6) functions, respectively, and their gradients. It is important to observe that the performance of the obtained method is influenced by the target optimization function. Remember that the MMSE-IRC function was used to calculate the final quality measure. As a result, the "IRC" method, which optimises the target function directly, has a higher final quality measure.

On the other hand, the "CD" method, on the other hand, converges faster through iterations and each iteration is computationally simpler than IRC. On the Fig. 3 one can find the quality of the proposed gradient methods by iterations. We noticed that modification of algorithm that uses approximated "CD" optimization function gives better results than "IRC" target function in the first iterations. At higher iterations the "IRC" gradient method superiors the "CD" method.

The third keyword in the title of gradient methods, "RZF" (18) and "ARZF" (19), refers to the method's starting point. The method will be more convergent if the starting point is better. Methods based on the "ARZF" starting point outperform methods based on the "RZF" point in this way. Remember that our issue isn't concave. As a result, we only find the local maximum, and a good starting point is critical for our method to work.

## 5. Conclusion

The paper studies the multi-user precoding problem as a non-convex optimization problem for wireless MIMO systems. In this study we approximate the Spectral Efficiency objective function using a differentiable projection-based method, where gradients are taken both for the function and the projection, which tends to very fast convergence of the proposed

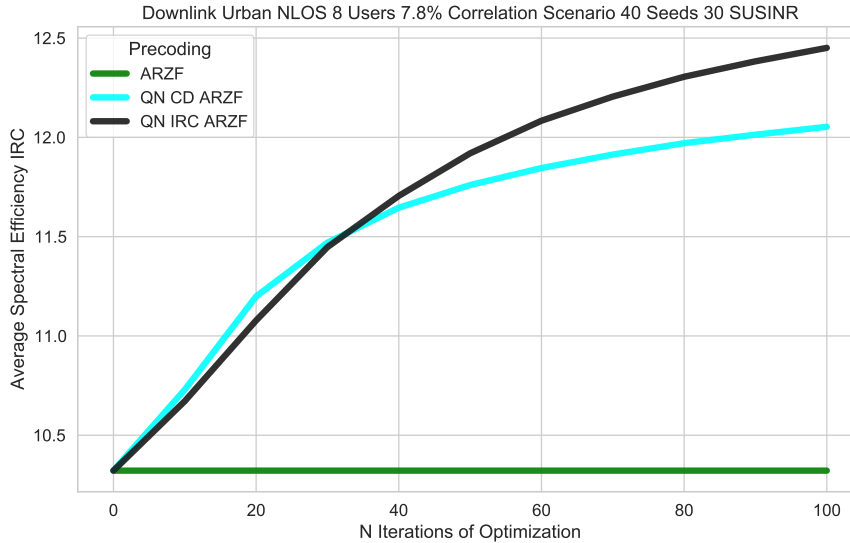


Figure 3. Urban NLOS 8 Users. The graph shows IRC Spectral Efficiency of the different precoding algorithms.

Precoding <i>SUSINR</i>	MRT	ZF	RZF	ARZF	QN CD RZF	QN CD ARZF	QN IRC RZF	QN IRC ARZF
-4	0.60	0.26	0.59	1.58	1.92	1.92	2.13	2.10
0	0.79	0.52	0.85	2.25	2.70	2.69	2.95	2.95
4	0.98	0.95	1.24	3.02	3.59	3.64	3.91	3.94
8	1.16	1.56	1.78	3.89	4.59	4.70	4.99	5.00
12	1.33	2.38	2.52	4.86	5.73	5.85	6.17	6.20
16	1.51	3.39	3.46	5.90	6.92	7.11	7.42	7.47
20	1.70	4.57	4.61	7.04	8.17	8.42	8.71	8.81
24	1.91	5.93	5.95	8.29	9.43	9.83	10.01	10.25
28	2.11	7.41	7.42	9.59	10.67	11.28	11.25	11.68
32	2.29	9.15	9.15	11.06	11.99	12.80	12.57	13.18
36	2.45	11.06	11.06	12.63	13.53	14.35	13.97	14.64
40	2.56	13.14	13.14	14.31	15.28	15.90	15.45	16.08

Table 2. Urban NLOS 8 Users. The table shows IRC Spectral Efficiency of the different precoding algorithms.

method. We then reduce the precoding problem to an unconstrained optimization task and solve it by the Quasi-Newton L-BFGS iterative procedure. Finally, all our research is based on realistic power limits per antenna and multiple antenna users, which in itself is a standalone problem for finding the right approach to solving. All investigated algorithms were studied in massive experiments using Quadriga software. The proposed method shows monotonic improvement over heuristic methods with reasonable computation time. It has a simple implementation and can be a good reference for other heuristic algorithms in the MIMO field.

## Acknowledges

Authors are very grateful for D. Minenkov for fruitful discussions.

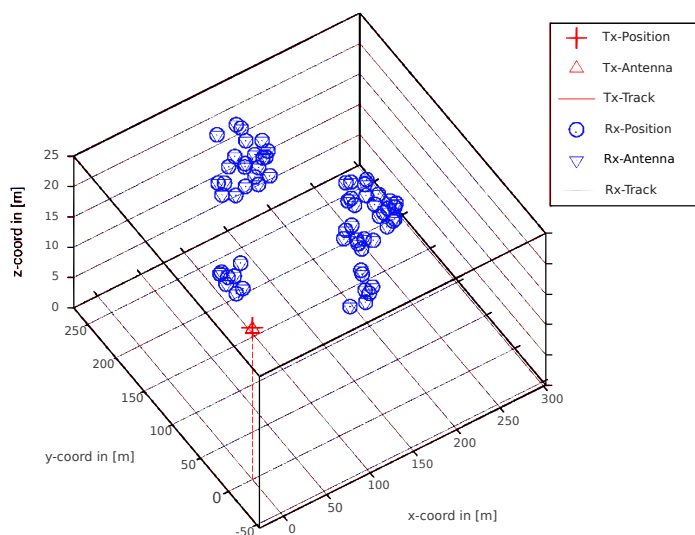


Figure 4. Example of Users for Urban Two Building Setup [2] .

Parameter	Value
Base station parameters	
number of base stations	1
position, m: (x, y, z) axes	(0, 0, 25)
number of antenna placeholders (y axis)	8
number of antenna placeholders (z axis)	4
distance between placeholders (y axis)	0.5 wavelength
distance between placeholders (z axis)	1.7 wavelength
antenna model	3gpp-macro
half-Power in azimuth direction, deg	60
half-Power in elevation direction, deg	10
front-to back ratio, dB	20
total number of antennas	64
Receiver parameters	
number of placeholders at the receiver (x axis)	2
distance between placeholders (x axis)	0.5 wavelength
antenna model	half-wave-dipole
total number of antennas	4
Quadriga simulation parameters	
central band frequency	3.5 GHz
1 sample per meter (default value)	1
include delay of the LOS path	1
disable spherical waves (use_3GPP_baseline)	1
Quadriga channel builders parameters	
shadow fading sigma	0
cluster splitting	False
bandwidth	100 MHz
number of subcarriers	42

Table 3. Quadriga generation parameters.

## References

- [1] E. Björnson, J. Hoydis, and L. Sanguinetti, *Massive mimo networks: Spectral, energy, and hardware efficiency*, Foundations and Trends in Signal Processing 11 (2017), pp. 154–655.
- [2] E. Bobrov, B. Chinyaev, V. Kuznetsov, H. Lu, D. Minenkov, S. Troshin, D. Yudakov, and D. ZaeV, *Adaptive regularized zero-forcing beamforming in massive mimo with multi-antenna users*, arXiv preprint arXiv:2107.00853 (2021).
- [3] F. Bohagen, P. Orten, and G. Oien, *Construction and capacity analysis of high-rank line-of-sight MIMO channels*, in *IEEE Wireless Communications and Networking Conference, 2005*, Vol. 1, 2005, pp. 432–437.
- [4] J.C. Chen, *Gradient projection-based alternating minimization algorithm for designing hybrid beamforming in millimeter-wave mimo systems*, IEEE Communications Letters 23 (2018), pp. 112–115.
- [5] H.H. Dam and A. Cantoni, *Interior point method for optimum zero-forcing beamforming with per-antenna power constraints and optimal step size*, Signal processing 106 (2015), pp. 10–14.
- [6] L. Garcia-Ordóñez, D.P. Palomar, A. Pages-Zamora, and J.R. Fonollosa, *Analytical BER performance in spatial multiplexing MIMO systems*, in *IEEE 6th Workshop on Signal Processing Advances in Wireless Communications, 2005.*, 2005, pp. 460–464.
- [7] S. Jaeckel, L. Raschkowski, K. Börner, and L. Thiele, *Quadriga: A 3-d multi-cell channel model with time evolution for enabling virtual field trials*, IEEE Transactions on Antennas and Propagation 62 (2014), pp. 3242–3256.
- [8] M. Joham, W. Utschick, and J.A. Nossek, *Linear transmit processing in mimo communications systems*, IEEE Transactions on signal Processing 53 (2005), pp. 2700–2712.
- [9] T.K. Lo, *Maximum ratio transmission*, in *1999 IEEE international conference on communications (Cat. No. 99CH36311)*, Vol. 2, 1999, pp. 1310–1314.
- [10] A.H. Mehana and A. Nosratinia, *Diversity of mmse mimo receivers*, IEEE Transactions on information theory 58 (2012), pp. 6788–6805.
- [11] L.D. Nguyen, H.D. Tuan, T.Q. Duong, and H.V. Poor, *Multi-user regularized zero-forcing beamforming*, IEEE Transactions on Signal Processing 67 (2019), pp. 2839–2853.
- [12] C.B. Peel, B.M. Hochwald, and A.L. Swindlehurst, *A vector-perturbation technique for near-capacity multiantenna multiuser communication-part i: channel inversion and regularization*, IEEE Transactions on Communications 53 (2005), pp. 195–202.
- [13] B. Ren, Y. Wang, S. Sun, Y. Zhang, X. Dai, and K. Niu, *Low-complexity mmse-irc algorithm for uplink massive mimo systems*, Electronics Letters 53 (2017), pp. 972–974.
- [14] S. Shi, M. Schubert, and H. Boche, *Downlink mmse transceiver optimization for multiuser mimo systems: Duality and sum-mse minimization*, IEEE Transactions on Signal Processing 55 (2007), pp. 5436–5446.
- [15] L. Sun and M.R. McKay, *Eigen-based transceivers for the mimo broadcast channel with semi-orthogonal user selection*, IEEE Transactions on Signal Processing 58 (2010), pp. 5246–5261.
- [16] S. Verdú, *Spectral efficiency in the wideband regime*, IEEE Transactions on Information Theory 48 (2002), pp. 1319–1343.
- [17] Z. Wang and W. Chen, *Regularized zero-forcing for multiantenna broadcast channels with user selection*, IEEE Wireless Communications Letters 1 (2012), pp. 129–132.
- [18] A. Wiesel, Y.C. Eldar, and S. Shamai, *Zero-forcing precoding and generalized inverses*, IEEE Transactions on Signal Processing 56 (2008), pp. 4409–4418.
- [19] D. Wubben, R. Bohnke, V. Kuhn, and K.D. Kammeyer, *Near-maximum-likelihood detection of MIMO systems using MMSE-based lattice-reduction*, in *2004 IEEE International Conference on Communications (IEEE Cat. No. 04CH37577)*, Vol. 2, 2004, pp. 798–802.
- [20] T. Yoo and A. Goldsmith, *On the optimality of multiantenna broadcast scheduling using zero-forcing beamforming*, IEEE Journal on selected areas in communications 24 (2006), pp. 528–541.
- [21] W. Yu and T. Lan, *Transmitter optimization for the multi-antenna downlink with per-antenna power constraints*, IEEE Transactions on signal processing 55 (2007), pp. 2646–2660.
- [22] C. Zhu, R.H. Byrd, P. Lu, and J. Nocedal, *Algorithm 778: L-bfgs-b: Fortran subroutines for large-scale bound-constrained optimization*, ACM Transactions on mathematical software (TOMS) 23 (1997), pp. 550–560.